IEEE Access
Multidisciplinary | Rapid Review | Open Access Journal

Received January 20, 2022, accepted January 30, 2022, date of publication February 1, 2022, date of current version February 10, 2022.

Digital Object Identifier 10.1109/ACCESS.2022.3148391

A New Algorithm for Displaying Images With High Resolution Using a Directional Volumetric Display With Threads and a Projector

TOMOYA IMAMURA[1], MITSURU BABA[1], NAOTO HOSHIKAWA[2], (Member, IEEE), HIROTAKA NAKAYAMA[3], TOMOYOSHI ITO[1], AND ATSUSHI SHIRAKI[1,4]

[1]Graduate School of Engineering, Chiba University, Chiba 263-8522, Japan
[2]Department of Innovative Electrical and Electronic Engineering, Oyama College, National Institute of Technology, Oyama 323-0806, Japan
[3]Center for Computational Astrophysics, National Astronomical Observatory of Japan, Mitaka, Tokyo 181-8588, Japan
[4]Institute of Management and Information Technologies, Chiba University, Chiba 263-8522, Japan

Corresponding author: Atsushi Shiraki (ashiraki@chiba-u.jp)

This work was supported in part by the Yazaki Memorial Foundation for Science and Technology.

ABSTRACT Using threads and a projector, a directional volumetric display capable of moving images and full-color representation was developed in our previous work. However, the horizontal resolution of the directional volumetric display could only achieve 20 pixels with 400 threads. Further, the conventional algorithm requires P squared threads per P horizontal pixels of the input image. Because it is difficult to place a large number of threads, thus, a new algorithm for developing projected images to improve the directional volumetric display's resolution was proposed. It is feasible to display images of P pixels with at least P threads using this technique. However, the higher the resolution, the lower the image quality in the proposed algorithm. Thus, it was verified how many threads can be used to display high-resolution images without degrading the image quality. Further, by representing the horizontal resolution of the input image with 5-6 threads per pixel, it is possible to display high-resolution images while maintaining the image quality. The proposed technique can display 64 pixels per 384 threads, whereas the conventional method can only display 20 pixels input images per 400 threads.

INDEX TERMS Volumetric display, directional display, interactive display, high resolution.

I. INTRODUCTION

Several three-dimensional (3D) display technologies such as holography [1], [2] have been developed recently. Holography is an ideal 3D display technology that can record and reproduce 3D information in its original form. However, the computational complexity of holograms for capturing three-dimensional information has been a major concern. Custom hardware accelerators such as field-programmable gate arrays (FPGAs) and ASICs (application-specific integrated circuits) for high-speed computing [3], [4] have recently been shown to offer a feasible solution to this problem. Another type of 3D display technology is a volumetric display [5]–[7]; it is a technology that uses water drops, bubbles, plasma, and rotating objects as a medium [8]–[11] to show images on a volumetric display. Volumetric displays using photophoretic trapping, which can display full-color images in the air [12], [13], and a volumetric display using a femtosecond laser and two parabolic mirrors facing each other [14], and multimodal acoustic trapping displays, capable of trapping particles acoustically and delivering visual, auditory, and tactile contents simultaneously [15], have recently been developed.

Nakayama *et al.* [16] proposed simultaneously displaying different two-dimensional information for multiple directions using a volumetric display. A display produced through this technique is called a directional volumetric display because it conveys information in a specific viewpoint direction (Figure 1). Directional volumetric displays are currently being developed using 3D crystals, light-emitting diodes (LEDs), quantum dots (QDs), inkjet printing, and threads [16]–[20]. Figure 1(a) shows a directional volumetric display using 3D crystals, and Figure 1(b) shows a directional volumetric display using threads and a projector.

The associate editor coordinating the review of this manuscript and approving it for publication was Sunil Karamchandani.

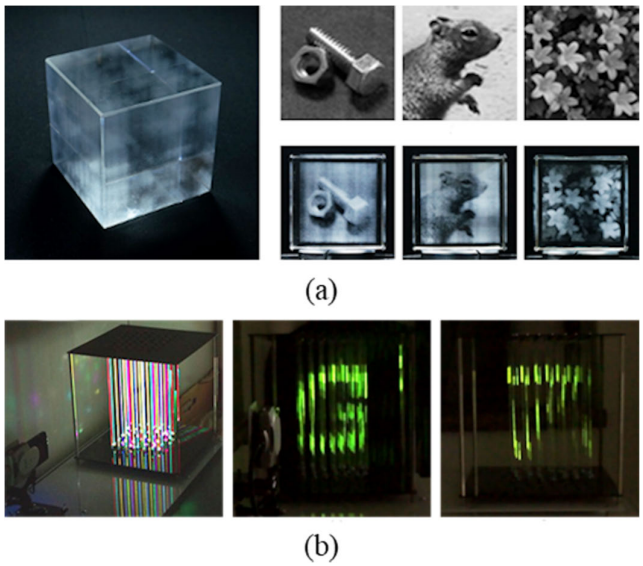

FIGURE 1. Directional volumetric display: (a) using 3D crystal, (b) using threads and a projector [16].

It is now possible to display higher resolution images using threads instead of LEDs.

Further, the directional volumetric display has been researched to develop interactive displays for people and systems. These include systems that transmit images while following the observer and systems that display directional images based on the language and position of the observer [21], [22]. Thus, the directional volumetric display is expected to be used for both practical and entertaining purposes. However, there are limitations, such as the display of low horizontal resolution. Threads must be added to increase the resolution, but the cost rises exponentially as the resolution increases. When the horizontal resolution of the displayed image is P, the thread to the square of P is required. Thus, a new design algorithm to achieve high resolution is proposed in this study.

The main contributions of this study are as follows.

- P threads are required per pixel of the horizontal resolution of the displayed image in the conventional method, but it is confirmed that the number of threads can be reduced to 1 per pixel of the horizontal resolution of the displayed image in this method.
- It was shown that the image quality was almost equal to that of the conventional method with 5-6 threads per pixel in the horizontal direction of the displayed image.
- Contrary to the conventional method, which displays an image of 20 $\times$ 20 pixels with 400 threads, this method displays an image of 64 $\times$ 64 pixels with almost the same number of threads.

The technologies for displaying different images depending on the viewing direction are introduced in Section II, the method achieving high resolution of the directional volumetric display is described in Section III, and the results and discussions are described in Sections IV and V, respectively. Finally, the conclusion and future work are described.

II. RELATED WORK

Viewpoint-dependent viewing can be accomplished by several techniques. Pjanic *et al.* [23] and Sakurai *et al.* [24] developed a technique for creating color patterns with varying hues when viewed from a different perspective. Ikeda *et al.* also developed a system that uses a high-speed projector at 2,400 frames per second to project a specific image on a flat surface, which displays different images based on movement at a specific speed and direction [25]. However, these techniques have limitations as multiple images can only be displayed on flat surfaces.

The objects on the cover of ''Gödel, Escher, Bach: An Eternal Golden Braid'' and ''The SQRIANCLE'' (coined from Square, Triangle, Circle) are 3D objects that can be used to display multiple images in different directions [26], [27]. An example is ''Shadow Art'' developed by Mitra *et al.* [28]. Shadow Art creates a meaningful shape by shining light on the object from a specific angle and casting a shadow on the background. However, it is impossible to identify the object by looking at it directly. He developed a system model by inputting multiple target shadow images and projecting them as shadows to create a 3D model. To achieve this process, the user sets the light source's position, size, and orientation, and then uses the input images to hollow out the 3D model in its initial state. This allows multiple shadows to be projected from a single model formed. However, creating this Shadow Art is challenging because it cannot be expressed without a light source to cast the shadows. Further, Suzuki *et al.* proposed a method that uses wires to form user-specified line drawings from different viewpoints using two-line drawing images and a user-provided viewpoint as input [29]. Hsiao *et al.* recently developed a computational framework to automatically create multi-view 3D wire sculptures using two or three user-specified line drawings and their related viewpoints as input [30]. These methods do not require the creation of shadows because the shape can be determined by the wire itself; they do not illuminate the light source and it is easier to modify the sculpture than Shadow Art. The two-dimensional images projected from these three-dimensional objects are restricted to binary images, and the number of images displayed is severely restricted. It is also challenging to represent moving images. Thus, only simple objects such as characters and character silhouettes can be displayed.

Sugihara [31] realized topology-disturbing objects using optical illusion. Topology-disturbing objects are objects that appear to disturb topology when viewed from two specific viewpoints, such as two objects that appear to be separated from each other when viewed from one viewpoint but appear to cross each other when viewed from another viewpoint. In addition, Sugihara *et al.* [32] realized a 3D object that was initially incomplete but became complete when it was reinforced with specular reflection. The two-dimensional images

projected from these three-dimensional objects are restricted to binary images, and the number of images displayed is severely restricted. It is also challenging to represent moving images. Thus, only simple objects such as characters and character silhouettes can be displayed.

In our directional volumetric display, each voxel, which is a volume element consisting of a three-dimensional structure, has color information and gradation that can be displayed in full color. Multiple full-color movies can currently be displayed in different directions using threads and a projector. Further, a system that employs a directional volumetric display using threads and a projector to identify spoken languages and transmit the corresponding language has been developed. Thus, this can be a new information transmission system not only in the fields of art and entertainment but also in various scenarios because it can alleviate conventional limitations.

III. METHOD

A. CONVENTIONAL METHOD

As voxel generation method, consider a P × Q × R (horizontal × vertical × horizontal) virtual space, as shown in Figure 2. Using Shiraki *et al*'s method [33], the voxel value V_{ijk} of the volumetric display shown in the blue box is determined by adding the pixel values a_{ij} and b_{kj} of the input images to be displayed. Thus, the voxel value is given in Equation (1), where i, j, k are arbitrary coordinates of the system (x, y, z), and λ is a constant for normalizing the voxel values.

In the directional volumetric display using 3D crystals, the voxels are overlapping on the x- and z-axes, so adding them together from on the z-axis represents 1 pixel of the front image, and adding them on the x-axis represents 1 pixel of the side image. Therefore, the pixel value A_{ij} of the image observed from the front is expressed using Equation (2), and the pixel value B_{kj} of the image observed from the side is expressed using Equation (3).

The correspondence between voxels and threads in a directional volume display using threads is explained. Figure 3 (a) depicts a view of Figure 2 from the y-axis direction, with voxels overlapping in the y-axis direction. For each voxel, a thread is placed. Then, the voxel value calculated using Equation (1) is assigned to the corresponding height of the corresponding thread. Owing to the constraint of the thread arrangement, they do not overlap on the x- and z-axes, so 1 pixel of the front image is represented by binding R threads together from the x-axis direction. Similarly, a pixel in the side image is represented by binding P threads from the z-axis direction [20]. Figure 3 (b) shows the correspondence between the threads and displayed images. Four threads are bundled and observed to display one pixel in the horizontal direction of displayed images.

When displaying an image with a resolution of P × Q (horizontal × vertical) in the conventional method, P threads are used for each horizontal resolution of 1 pixel, and a total of P^2 threads are required for the entire display. As shown in Figure 3, four threads are used to display 1 pixel of the image, so only 4-pixel images can be displayed. Thus, the higher the resolution of the image, the higher the difficulty to fabricate the display.

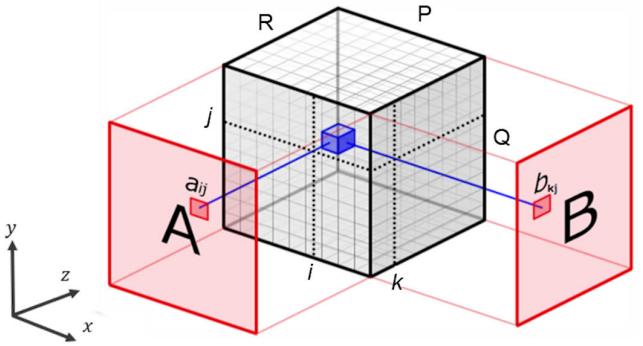

FIGURE 2. Voxel generation method.

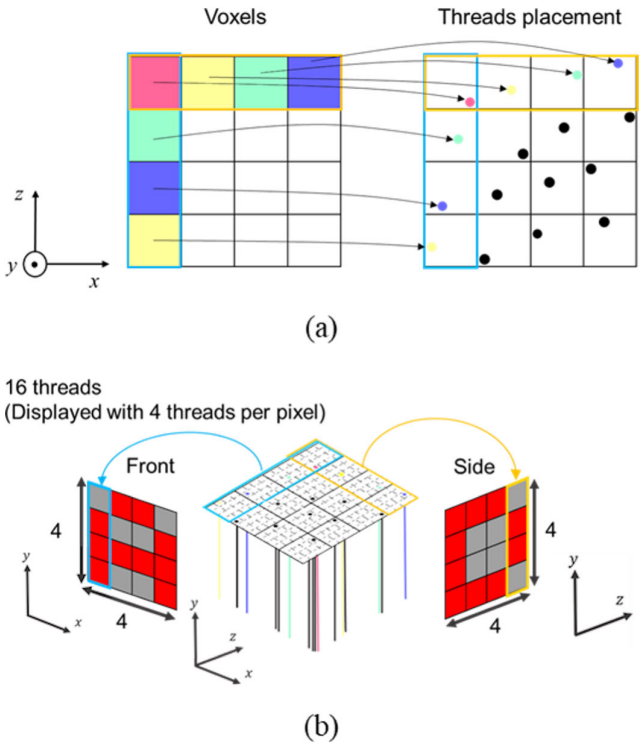

FIGURE 3. Conventional method: (a) assignment from voxel to thread, (b) correspondence between threads and display images.

$$V_{ijk} = \lambda(a_{ij} + b_{kj}). \tag{1}$$

$$A_{ij} = \sum_{k=1}^{R} V_{ijk}. \tag{2}$$

$$B_{kj} = \sum_{i=1}^{P} V_{ijk}. \tag{3}$$

B. PROPOSED METHOD

To achieve a higher resolution of the displayed image, reducing the number of threads required for 1 pixel in the horizontal

resolution by a factor of 1/N and allocating the reduced number of threads to a new horizontal resolution was proposed.

Equation (4) is used to determine the voxel value V of size P × Q × P generated from images PN × QN, which is N times expansion of the images displayed in the front and side views; where $a_{i'j}$ and $b_{k'j}$ are the pixel value of the image in the front and side views, respectively. Further, i, j, k is an arbitrary coordinate of the system (x, y, z), and λ is a constant for normalizing the voxel value.

$$V_{ijk} = \lambda(a_{i'j} + b_{k'j}). \tag{4}$$

The coordinates i' and k' of each image are calculated from Equations (5) and (6), where t_x and t_z are the coordinates of the thread placement in the x-z plane corresponding to each voxel. The range of the constant N depends on the number of threads required to display 1 pixel in the horizontal resolution of the images, and is expressed in Equation (7).

$$i' = t_x \times N + \frac{t_z}{\frac{P}{N} + 1}. \tag{5}$$

$$k' = t_z \times N + \frac{t_x}{\frac{P}{N} + 1}. \tag{6}$$

$$1 \leq N \leq P. \tag{7}$$

When the image is projected onto threads, a pixel of the front image is represented by binding P/N threads from the x-axis direction. A pixel of the side image is also represented using P/N threads bound from the z-axis direction. Figure 4 (a) depicts a view of Figure 2 from the y-axis direction, with voxels overlapping in the y-axis direction. Each thread is placed in each voxel that contains the coordinates calculated using Equations (5) and (6). Then, the voxel value calculated using Equation (4) is assigned to the corresponding height of the corresponding thread. Figure 4 (b) shows the correspondence between the threads and displayed images. Two threads are bundled and observed to display one pixel in the horizontal direction of the displayed images. In the conventional method (Figure 3), four threads are used to display 1 pixel of the image, so only 4-pixels images can be displayed. In this method, two threads are used to display one pixel of an image (Figure 4), so the image with eight pixels can be displayed.

This method allows the representation of images with a horizontal resolution of P pixel using P threads. However, reducing the number of threads reduces the projected image quality. Thus, how many threads per 1 pixel can be used to achieve high image quality while maintaining the input image quality is examined.

IV. RESULTS

A. EXPERIMENT

To verify the effectiveness of the proposed method, experiments were conducted. Figure 5 shows the relationship between the projector, threads, and observers. In Figure 6, the input images used in this study are 64 × 64 images. Input images were collected from "Standard Image / Sample Data" [34]. These can be used as standard images for simulation analysis. To obtain the simulation and projection results, the personal computer (PC) used was a Mac book pro (Apple Inc.). Table 1 shows the specifications of the PC, and Table 2 shows the information of the software used.

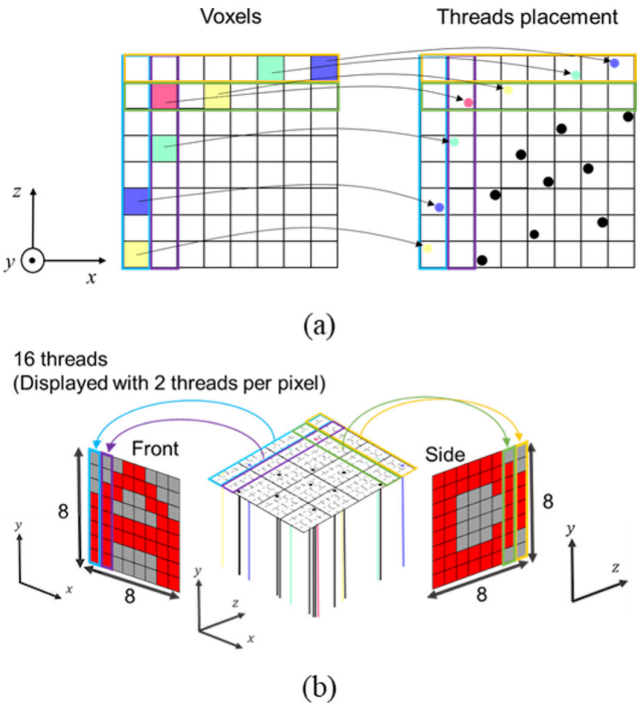

FIGURE 4. Proposed method (N = 2): (a) assignment from voxel to thread, (b) correspondence between threads and display images.

TABLE 1. The specifications of PC.

Central processing unit (CPU)	Intel Core i5 2.7-GHz dual-core
Memory	16 GB
Graphics processing unit (GPU)	Intel Iris Graphics 6100

Figures 6 (a) and (b) are used to form a projection image, which is then projected onto the threads to display Figure 6 (a) and (b) from the front and side views, respectively. Similarly, the projection image is created using Figures 6 (c) and (d), which are displayed from the front and side views, respectively. The simulation in this study is performed using multiple data of the number of threads, which is N times the resolution of the input images. In addition, although the simulation of threads would normally have a gap, the simulation image was generated with an ideal arrangement of threads with no gaps to facilitate the evaluation of image quality. The image quality of simulated images was evaluated using the peak signal-to-noise ratio (PSNR) and structural similarity (SSIM). PSNR is an image quality index that indicates how much noise is contained in a comparison image compared with the original image. SSIM is an image quality evaluation index that compares the luminance, contrast, and structure of a comparison and original images, and the higher the value, the higher is the image quality.

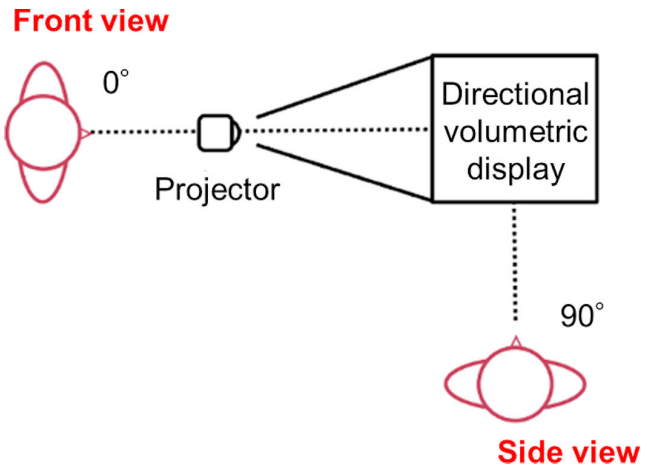

FIGURE 5. The relationship between a projector, threads, and observers.

TABLE 2. Information of the software.

Operating system	macOS Big Sur (version 11.6)
Programming language	C++17
Compiler	GNU C++ Compiler (version 13.0.0)
Compiler optimization options	-O3
Library	OpenCV 4.5.3

The evaluation using SSIM is said to be close to human perception. Mean absolute error (MAE) and mean square error (MSE), which are used in evaluating regression models, are used to analyze the error between the input image and simulation result. The closer MAE and MSE are to zero, the smaller the error and the closer the comparison image is to the input image. Further, the projected image was projected onto 64 threads and 384 threads, and the displayed image was observed.

B. RESULTS OF SIMULATION

Figure 7 shows the simulated image of the projection result. Figure 7 (a) shows the simulation result using the images in figures 6 (a) and (b), whereas figure 7 (b) depicts the result of the simulation using the images in figures 6 (c) and (d). The output results for 4,096 threads in Figure 7 are the conventional method's results. Table 3 shows the results of the evaluated output images using PSNR. Table 4 shows the results of the evaluated output images using SSIM. Table 5 shows the results of the evaluated output images using MAE. Table 6 shows the results of the evaluated output images using MSE.

From Figure 7, it is confirmed that this method can output high-resolution images. Further, from the results of the PSNR, SSIM, MAE, and MSE values, it can be confirmed that the image quality is poor when 64 threads are used, and improves as the number of threads increases. Furthermore, it is confirmed that the image quality when using more than 320 or 384 threads is almost equal to the image quality of the output image using 4,096 threads, which is the conventional method. Thus, it is feasible to display the image while

FIGURE 6. Original input images: (a-d) Images 1-4, respectively.

TABLE 3. PSNR values.

Number of threads	Figure 7 (a)		Figure 7 (b)	
	Front	Side	Front	Side
64	13.96	13.77	14.37	15.16
128	14.61	15.60	14.75	12.00
192	14.92	15.38	14.77	13.62
256	15.10	15.62	14.81	13.60
320	16.26	16.20	13.42	13.71
384	16.33	16.37	13.63	12.15
448	16.41	16.52	16.38	15.05
512	16.22	16.27	15.04	16.78
1,024	16.22	16.20	15.03	14.70
2,048	16.63	16.67	15.15	15.21
4,096	16.66	16.69	15.16	14.69

maintaining the image quality similar to the output images of the conventional method using 5 or 6 threads per 1 pixel of the original image's horizontal resolution.

C. RESULTS OF PROJECTION

Based on the simulation results, two types of directional volumetric displays, 64 and 384 threads, were fabricated, and projected images were projected onto the threads. The overview of the projection system for the directional volumetric display is shown in Figure 8. Images were projected using an MH550 projector (BenQ Japan Co., Ltd., Japan). The specifications of the projector are listed in Table 7. The projector was installed at a distance of 1.48 m from the directional volumetric display and 0.70 m above the floor. Vinymo MBT (Nagai Yoriito Co., Ltd., Japan) was used as the thread. The number of threads that constructed the directional volumetric display was 59 of 64 and 315 of 384. The failure to place the threads was that the constraints on thread placement of Shiraki *et al.* [20] could not be met.

Figure 9 shows the result of the projection onto 64 threads and Figure 10 shows the result of projecting onto 384 threads. Figures 9 (a), 9 (b), 10 (a), and 10 (b) show the result of the displayed images using the images in Figures 6 (a) and (b), and Figures 9 (c), 9 (d), 10 (c), and 10 (d) show the result of the displayed images using the images in Figures 6 (c) and (d). Figure 11 shows the results of observation from a direction other than the display direction (45°) when the projected images generated from Figures 6 (a) and (b) are projected onto 64 and 384 threads, respectively. Figures 11 (a) and (b) show the simulation results considering the position of the threads, whereas Figures 11 (c) and (d) show the projection results. Figures 11 (a) and (c) show the results of projection onto 64 threads, whereas Figures 11 (b) and (d) show the

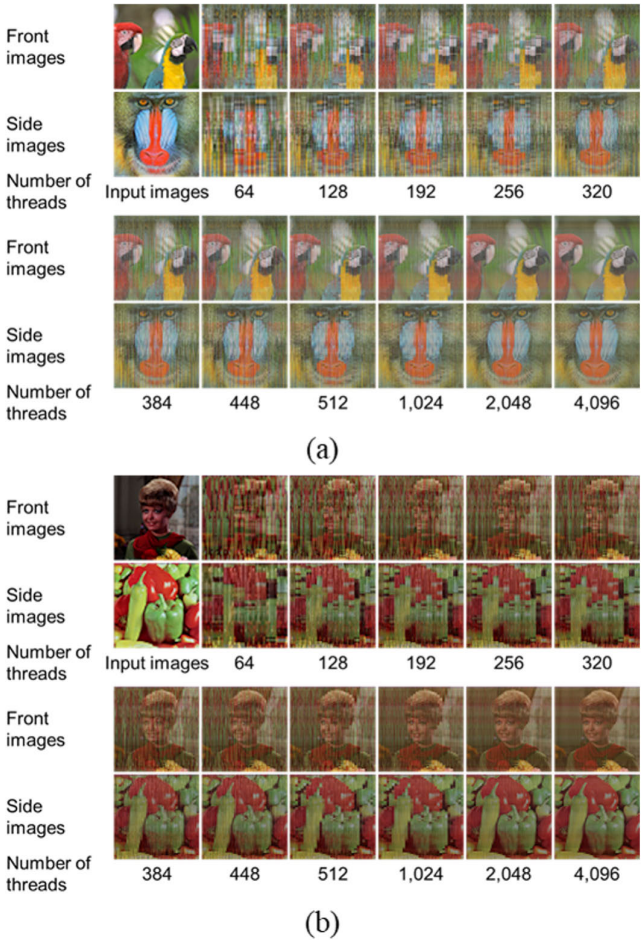

FIGURE 7. Input images and simulation results: (a) output images from Figures 6 (a) and (b); (b) output images from Figures 6 (c) and (d).

results of projection on 384 threads. Further, the video of the result of displaying the movies on 384 threads using the proposed method is shown in visualization 1. Moreover, the input movie for visualization 1 is created by Nakayama, the co-author.

Figures 9, 10 and visualization 1 show that different images can be observed in different directions. It was also confirmed from Figure 11 that the images could not be observed from other directions. The conventional method can only display images of 20 pixels (simple symbols and characters) with 400 threads [20], but the proposed method can display images of 64 pixels (more complex images) with 384 threads in Figure 10 and visualization 1.

V. DISCUSSION

This study compares the conventional and proposed methods, a comparison of input and simulated images, a comparison of projected and simulated results, and a discussion of the limitations of the proposed method were discussed.

A. COMPARISON OF THE PROPOSED METHOD AND THE CONVENTIONAL METHOD

To display multiple images, the pixel values of images displayed in different directions are added to the voxel calculation. The pixel values of images to be displayed in the other direction are errors and are included in all voxels. In the conventional method, all voxels, including the noise, are added in the depth direction to obtain the pixel values of displayed images. The noise is smoothed via adding voxels in the depth direction. This method reduces the number of voxels added in the depth direction and allocates the voxels to other pixels in the displayed image to achieve higher resolution.

Although there are differences in the results depending on the image used, Tables 3, 4, 5, and 6 show that the values of PSNR, SSIM, MAE, and MSE are low when the thread count is 64 because no smoothing is performed, and these values improve as the thread count increases. It was verified that using 5 to 6 threads per 1 pixel of the input image can be

TABLE 4. SSIM values.

Number of threads	Figure 7 (a)		Figure 7 (b)	
	Front	Side	Front	Side
64	0.1893	0.1532	0.1457	0.1467
128	0.2069	0.1896	0.1457	0.2302
192	0.2197	0.1694	0.0895	0.2032
256	0.2280	0.1733	0.1111	0.1985
320	0.2645	0.1839	0.1264	0.2430
384	0.2662	0.1919	0.1238	0.2458
448	0.2636	0.1979	0.1137	0.2402
512	0.2573	0.1806	0.1090	0.2314
1,024	0.2521	0.1814	0.1003	0.2270
2,048	0.2593	0.1916	0.1019	0.2355
4,096	0.2598	0.1922	0.1011	0.2353

TABLE 5. MAE values.

Number of threads	Figure 7 (a)		Figure 7 (b)	
	Front	Side	Front	Side
64	39.62	41.43	38.56	50.81
128	36.30	33.19	37.37	42.24
192	35.38	34.05	36.74	40.23
256	34.74	33.08	36.90	41.72
320	30.99	31.18	36.46	37.52
384	30.63	30.77	35.85	37.14
448	30.88	30.45	36.13	36.75
512	31.14	30.96	36.22	37.57
1,024	31.09	31.22	36.28	37.58
2,048	29.88	29.73	35.74	35.60
4,096	29.78	29.66	35.69	35.49

TABLE 6. MSE values.

Number of threads	Figure 7 (a)		Figure 7 (b)	
	Front	Side	Front	Side
64	2614.75	2728.44	2378.72	4130.47
128	2250.80	1792.35	2178.24	2826.22
192	2093.97	1883.27	2107.45	2546.75
256	2010.90	1782.39	2119.43	2758.02
320	1540.17	1558.55	2071.28	2196.17
384	1515.30	1498.63	2016.47	2146.30
448	1521.54	1482.53	2032.71	2099.58
512	1552.87	1536.10	2036.12	2204.53
1,024	1552.43	1559.09	2044.13	2206.72
2,048	1411.23	1398.03	1986.82	1960.03
4,096	1401.96	1392.58	1980.94	1949.99

TABLE 7. The specifications of MH550 projector.

Projection system	Digital Light
Brightness	3,500 ANSI Lumens
Resolution	1,920 × 1,080

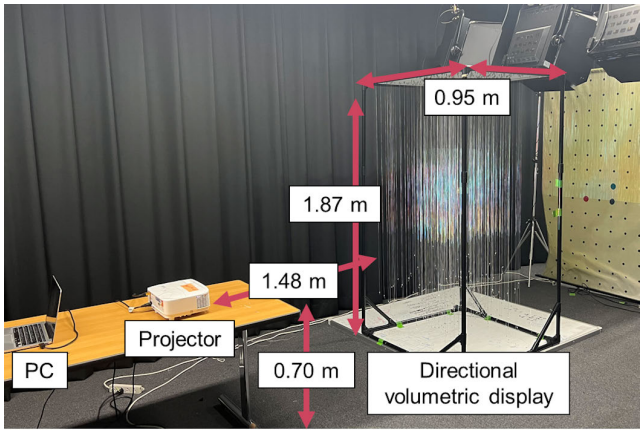

FIGURE 8. An overview of the projection system for the directional volumetric display.

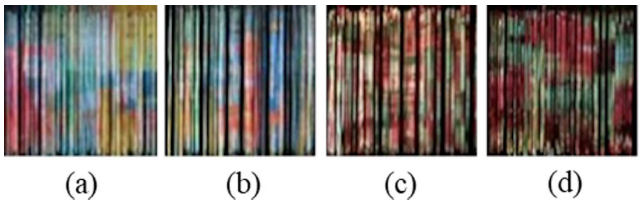

FIGURE 9. Displayed images (64 threads): (a, b) displayed images using Figures 6 (a) and (b); (c, d) displayed images using Figures 6 (c) and (d).

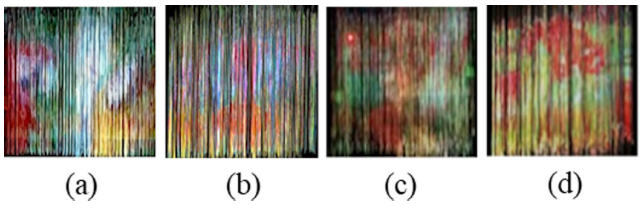

FIGURE 10. Displayed images (384 threads): (a, b) displayed images using Figures 6 (a) and (b); (c, d) displayed images using Figures 6 (c) and (d).

displayed while maintaining the image quality similar to the conventional method.

Finally, a comparison of the computational complexity of the conventional and proposed methods is presented. O-notation denotes the amount of computation. The computational complexity of the conventional and proposed methods depends on the number of voxels to be computed. In the conventional method, all voxels are computed, so the computational complexity is $\mathcal{O}(n^3)$. In this method, the number of voxels to be computed depends on the value of N in Equations (5) and (6), and the computational complexity changes. When N = 1, the computational complexity is $\mathcal{O}(n^3)$; however, the process is the same as the conventional method. When N $\neq$ 1, the computational complexity is $\mathcal{O}(n^2)$, which confirms that the proposed method is superior to the conventional method.

B. COMPARISON OF INPUT AND SIMULATION IMAGES

The values of PSNR, SSIM, MAE, and MSE improved as the number of threads increased, and it was confirmed that the image quality was equivalent to that of the conventional method at 320 or 384 threads. However, from Tables 3 and 4, it is confirmed that the PSNR and SSIM values do not increase, even when the number of threads increases. For example, in Figure 7 (a) in Tables 3 and 4, the values of PSNR and SSIM are larger when 384 threads are used than when 512 threads are used because the threads corresponding to noisy voxels are removed, which improve the image quality. Figure 7 (a) in Tables 5 and 6 also show that the values of MAE and MSE are smaller when 384 threads are used than when 512 threads are used. The MAE and MSE values are also smaller when 384 threads are used than when 512 threads are used because the threads corresponding to the noisy voxels are deleted.

In addition, when comparing Figures 7 (a) and (b) in Tables 3 and 4, it was observed that PSNR and SSIM differed depending on the combination of the two input images. For example, the front image in Figure 7 (b) has a lower SSIM value than the front image in Figure 7 (a) (Table 4). Further, Tables 5 and 6 show that the MAE and MSE values of the front and side images in Figure 7 (b) are larger than those of the frontal and side images in Figure 7 (a), and the errors are larger. This is because the current formulas used for voxel generation do not consider features such as the color tone and edges of the image; furthermore, the strength of the noise in the image that can be confirmed from the generated voxels depends largely on the combination of the images used for generation. Therefore, the image quality of the displayed image would depend on the combination of the thread arrangement and the input images.

C. COMPARISON OF PROJECTION RESULT AND SIMULATION IMAGES

The displayed images of the projection results in Figures 9 and 10 were close to the results of the simulation with 64 and 384 threads in Figure 7. It was also confirmed from Figure 11 that the image could not be observed from any direction other than the display direction. However, there is some error between the projection results in Figures 9 and 10 and the results of the simulation with 64 and 384 threads in Figure 7.

The following are two reasons for the discrepancy between the projected and simulated results: (1) The thread is placed manually, resulting in an error between the placement of the thread in the simulation and the placement of the actual hanging thread. Thus, threads obstruct the rays, which should not hit it, resulting in noise. To address this issue, it is

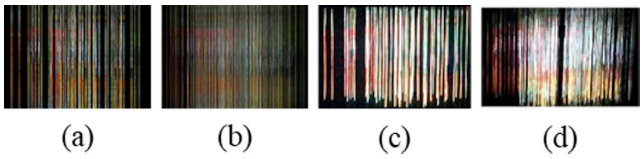

FIGURE 11. The observation results of undesignated viewing position (45°) using Figures 6 (a) and (b): (a, b) simulation images; (c, d) projected images; (a, c) using 64 threads; (b, d) using 384 threads.

crucial to place the threads accurately, but this is not practical. (2) The brightness of the projected and the simulated images are similar, thus when the image is projected, the brightness value changes depending on the reflectance of the thread, which is assumed to be different from the actual simulation result. To address this issue, it is important to consider the reflectance of the projected object. Huang *et al.* [35], [36] previously succeeded in projecting an image similar to the actual input image by correcting the input image using the information on the projection surface captured by a camera and an ambient light. The camera used in this study was only for capturing the projection results. In the future, it is necessary to use a camera to obtain projection surface information and realize projection based on the information of the projection surface, thereby reducing the error with the simulation results.

D. LIMITATIONS

It was confirmed that by representing each pixel of the input image with 5-6 threads of horizontal resolution, the image quality of the displayed image was almost equal to that of the conventional method. A directional volumetric display capable of displaying (256 × 256)-pixel images is considered to be fabricated using approximately 1,500 threads. Currently, images of 4-5 pixels per thread are projected using a projector. Therefore, when using a projector capable of projecting an image of 1,920 × 1,080 pixels, the number of threads that can project an image is approximately 400. So, to project images onto 1,500 threads, it is necessary to reduce the number of pixels of the image projected onto each thread or increase the number of projectors that project the image.

The video in visualization 1 takes an average of 0.15 s to create a single projected image and can display only approximately 6.6 frames per second. In addition, as the resolution increases, the time required to create a projected image increases, so in the future, using input images with 256 × 256 pixels will take 16 times longer than using input images with 64 × 64 pixels. When considering a display at 30 frames per second, the projection image generation would need to be approximately five times faster when using a 64-pixel input image. Similarly, when input images with 256 × 256 pixels are used, the acceleration is approximately 80 times.

To realize an interactive directional volumetric display that updates the displayed image according to the observer's observation position, directional displays to 0° and 30°, 0° and 60°, and 0° and 90° were simulated using 384 threads. The results are shown in Figure 12. Figures 12 (a), (b), (c), and (d) show the simulation results of displaying images at 0° and 30°, Figures 12 (e), (f), (g), and (h) show simulation results of displaying images at 0° and 60°, and Figures 12 (i), (j), (k), and (l) show simulation results of displaying images at 0° and 90°. Figures 12 (a), (e), and (i) are the results of observing the image from 0°, Figures 12 (b), (f), and (j) are the results of observing the image from 30°, Figures 12 (c), (g), and (k) are the results of observing the image from 60°, and Figures 12 (d), (h), and (l) are the results of observing the image from 90°. However, when the directional volumetric display is observed from a position other than the front and side directions, the overlapping of threads and the expansion and shrinkage of the display size in the horizontal direction cause a loss of the displayed image. This is because the proposed method only optimizes the placement of threads in the 0° and 90° directions owing to reducing the number of threads assigned to each pixel. Therefore, it is necessary to develop a model based on this method to place the threads so that the quality of the displayed image is maintained uniformly, regardless of the viewing direction.

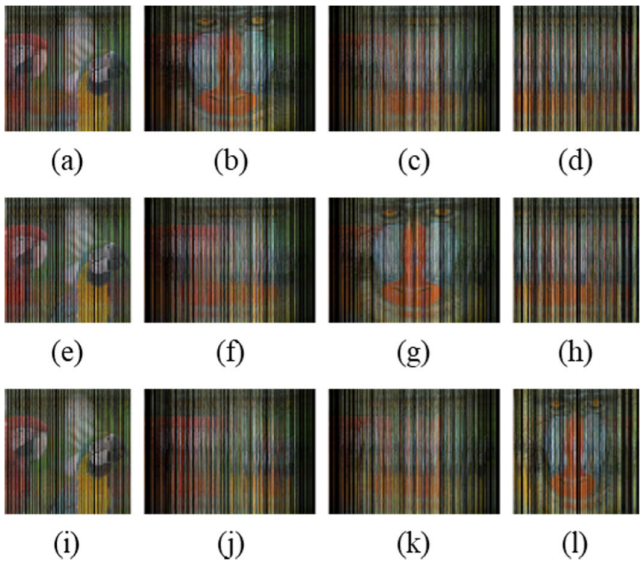

FIGURE 12. Simulation results of displaying images in four directions (384 threads): (a-d) simulation results of displaying images at 0° and 30°; (e-h) simulation results of displaying images at 0° and 60°; (i-l) simulation results of displaying images at 0° and 90°; (a, e, j) results of observing the image from 0°, (b, f, j) results of viewing the image from 30°; (c, g, k) results of observing the image from 60°;(d, h, l) results of observing the image from 90°.

VI. CONCLUSION AND FUTURE WORK

This study proposes and validates a new design algorithm to improve the resolution of a directional volumetric display using threads and a projector. The conventional method requires threads of the square of the horizontal resolution to build a directional volumetric display, whereas the proposed method represents the directional volumetric display with

threads of at least the horizontal resolution. By representing each pixel of the input image with 5-6 threads of horizontal resolution, it was confirmed that the image quality of the displayed image was almost the same as that of the conventional method.

In the future, with the goal of practical application in the entertainment field, the aim is to fabricate a directional volumetric display capable of displaying (256 × 256)-pixel images with approximately 1,500 threads. As described in Subsection V-D, to fabricate the directional volumetric display capable of displaying images of 256 × 256 pixels, it is necessary to reduce the number of pixels projected on each thread or increase the number of projectors that project images. However, in the former case, the resolution cannot be higher than the projector's performance (1,920 × 1,080 pixels). In addition, although there are projectors that can display images with higher resolution than 1,920 × 1,080 pixels, they are expensive. Therefore, a directional volumetric display that displays images with 256 × 256 pixels will be realized by projecting images using multiple projectors.

In this study, only the CPU was used to generate projected images. Matsumoto *et al.* [21] achieved an acceleration of up to 27.45 times faster than using only the CPU using NVIDIA GeForce GTX 1050 GPU in generating projected images when using a 64-pixel input image. Therefore, using a high-performance GPU, such as NVIDIA GeForce RTX 3090, to generate projected images, it may be possible to display (256 × 256)-pixel images at 30 frames per second. Further, a new interactive system will be developed using a directional volumetric display to present multimedia.

REFERENCES

[1] P. St-Hilaire, S. A. Benton, M. Lucente, M. L. Jepsen, J. Kollin, H. Yoshikawa, and J. Underkoffler, "Electronic display system for computational holography," *Proc. SPIE*, vol. 1212, pp. 174–182, May 1990, doi: 10.1117/12.17980.

[2] P. S. Hilaire, S. A. Benton, M. Lucente, J. D. Sutter, and W. J. Plesniak, "Advances in holographic video," *Proc. SPIE*, vol. 1914, pp. 188–196, Sep. 1993, doi: 10.1117/12.155020.

[3] T. Sugie, T. Akamatsu, T. Nishitsuji, R. Hirayama, N. Masuda, H. Nakayama, Y. Ichihashi, A. Shiraki, M. Oikawa, N. Takada, Y. Endo, T. Kakue, T. Shimobaba, and T. Ito, "High-performance parallel computing for next-generation holographic imaging," *Nature Electron.*, vol. 1, pp. 254–259, Apr. 2018, doi: 10.1038/s41928-018-0057-5.

[4] Y. Wang, D. Dong, P. J. Christopher, A. Kadis, R. Mouthaan, F. Yang, and T. D. Wilkinson, "Hardware implementations of computer-generated holography: A review," *Opt. Eng.*, vol. 59, no. 10, pp. 1–15, Feb. 2020, doi: 10.1117/1.OE.59.10.102413.

[5] B. G. Blundell, A. J. Schwarz, and D. K. Horrell, "Volumetric three-dimensional display systems: Their past, present and future," *Eng. Sci. Educ. J.*, vol. 2, no. 5, pp. 196–200, Oct. 1993, doi: 10.1049/esej:19930058.

[6] D. L. MacFarlane, "Volumetric three-dimensional display," *Appl. Opt.* vol. 33, no. 31, pp. 7453–7457, Nov. 1994, doi: 10.1364/AO.33.007453.

[7] G. E. Favalora, "Volumetric 3D displays and application infrastructure," *Computer*, vol. 38, no. 8, pp. 37–44, Aug. 2005, doi: 10.1109/MC.2005.276.

[8] S. Eitoku, T. Tanikawa, and Y. Suzuki, "Display composed of water drops for filling space with materialized virtual three-dimensional objects," in *Proc. IEEE Virtual Reality Conf.*, Mar. 2006, pp. 159–166, doi: 10.1109/VR.2006.51.

[9] Y. Ochiai, K. Kumagai, T. Hoshi, J. Rekimoto, S. Hasegawa, and Y. Hayasaki, "Fairy lights in femtoseconds: Aerial and volumetric graphics rendered by focused femtosecond laser combined with computational holographic fields," *ACM Trans. Graph.*, vol. 35, no. 2, pp. 1–14, May 2016, doi: 10.1145/2850414.

[10] K. Kumagai, S. Hasegawa, and Y. Hayasaki, "Volumetric bubble display," *Optica*, vol. 4, no. 3, pp. 298–302, Feb. 2017, doi: 10.1364/OPTICA.4.000298.

[11] M. Gately, Y. Zhai, M. Yeary, E. Petrich, and L. Sawalha, "A three-dimensional swept volume display based on LED arrays," *J. Display Technol.*, vol. 7, no. 9, pp. 503–514, Sep. 2011, doi: 10.1109/JDT.2011.2157455.

[12] D. E. Smalley, E. Nygaard, K. Squire, J. Van Wagoner, J. Rasmussen, S. Gneiting, K. Qaderi, J. Goodsell, W. Rogers, M. Lindsey, K. Costner, A. Monk, M. Pearson, B. Haymore, and J. Peatross, "A photophoretic-trap volumetric display," *Nature*, vol. 553, no. 7689, pp. 486–490, Jan. 2018, doi: 10.1038/nature25176.

[13] W. Rogers and D. Smalley, "Simulating virtual images in optical trap displays," *Sci. Rep.*, vol. 11, Apr. 2021, Art. no. 7522, doi: 10.1038/s41598-021-86495-6.

[14] K. Kumagai, S. Miura, and Y. Hayasaki, "Colour, volumetric display based on holographic-laser-excited graphics using drawing space separation," *Sci. Rep.*, vol. 11, Nov. 2021, Art. no. 22728, doi: 10.1038/s41598-021-02107-3.

[15] R. Hirayama, D. M. Plasencia, N. Masuda, and S. Subramanian, "A, volumetric display for visual, tactile and audio presentation using acoustic trapping," *Nature*, vol. 575, pp. 320–323, Nov. 2019, doi: 10.1038/s41586-019-1739-5.

[16] H. Nakayama, A. Shiraki, R. Hirayama, N. Masuda, T. Shimobaba, and T. Ito, "Three-dimensional, vol. containing, multiple two-dimensional information patterns," *Sci. Rep.*, vol. 3, Jun. 2013, Art. no. 1931, doi: 10.1038/srep01931.

[17] R. Hirayama, A. Shiraki, H. Nakayama, T. Kakue, T. Shimobaba, and T. Ito, "Operating scheme for the light-emitting diode array of a volumetric display that exhibits multiple full-color dynamic images," *Opt. Eng.*, vol. 56, no. 7, Jul. 2017, Art. no. 073108, doi: 10.1117/1.OE.56.7.073108.

[18] R. Hirayama, M. Naruse, H. Nakayama, N. Tate, A. Shiraki, T. Kakue, T. Shimobaba, M. Ohtsu, and T. Ito, "Design, implementation and characterization of a quantum-dot-based, volumetric display," *Sci. Rep.*, vol. 5, Feb. 2015, Art. no. 8472, doi: 10.1038/srep08472.

[19] R. Hirayama, T. Suzuki, T. Shimobaba, A. Shiraki, M. Naruse, H. Nakayama, T. Kakue, and T. Ito, "Inkjet printing-based, volumetric display projecting multiple full-colour 2D patterns," *Sci. Rep.*, vol. 7, Apr. 2017, Art. no. 46511, doi: 10.1038/srep46511.

[20] A. Shiraki, M. Ikeda, H. Nakayama, R. Hirayama, T. Kakue, T. Shimobaba, and T. Ito, "Efficient method for fabricating a directional volumetric display using strings displaying multiple images," *Appl. Opt.*, vol. 57, no. 1, pp. A33–A38, Jan. 2018, doi: 10.1364/AO.57.000A33.

[21] D. Matsumoto, R. Hirayama, N. Hoshikawa, H. Nakayama, T. Shimobaba, T. Ito, and A. Shiraki, "Interactive directional volumetric display that keeps displaying directional image only to a particular person in real-time," *OSA Continuum*, vol. 2, no. 11, pp. 3309–3322, Nov. 2019, doi: 10.1364/OSAC.2.003309.

[22] M. Baba, T. Imamura, N. Hoshikawa, H. Nakayama, T. Ito, and A. Shiraki, "Development of a multilingual digital signage system using a directional volumetric display and language identification," *OSA Continuum*, vol. 3, no. 11, pp. 3187–3196, Nov. 2020, doi: 10.1364/OSAC.405929.

[23] P. Pjanic and R. D. Hersch, "Color changing effects with anisotropic halftone prints on metal," *ACM Trans. Graph.*, vol. 34, no. 6, Oct. 2015, Art. no. 167, doi: 10.1145/2816795.2818083.

[24] K. Sakurai, Y. Dobashi, K. Iwasaki, and T. Nishita, "Fabricating reflectors for displaying multiple images," *ACM Trans. Graph.*, vol. 37, no. 4, Jul. 2018, Art. no. 158, doi: 10.1145/3197517.3201400.

[25] H. Ikeda, T. Hayakawa, and M. Ishikawa, "Bilateral motion display: Strategy to provide multiple visual perception using afterimage effects for specific motion," in *Proc. 25th ACM Symp. Virtual Reality Softw. Technol.*, vol. 17, Nov. 2019, pp. 1–5, doi: 10.1145/3359996.3364241.

[26] D. R. Hofstadter, *Gödel, Escher, Bach: An Eternal Golden Braid*. New York, NY, USA: Basic Books, 1979.

[27] G. Sela and G. Elber, "Generation of view dependent models using free form deformation," *Vis. Comput.*, vol. 23, no. 3, pp. 219–229, Jan. 2007, doi: 10.1007/s00371-006-0095-2.

[28] N. J. Mitra and M. Pauly, "Shadow art," *ACM Trans. Graph.*, vol. 28, no. 5, pp. 1–7, Dec. 2009, doi: 10.1145/1661412.1618502.

[29] R. Suzuki, M. Moriguchi, and K. Imai, "Generation and optimization of multi-view wire art," in *Proc. 25th Pacific Conf. Comput. Graph. Appl.*, Taipei, Taiwan, Oct. 2017, pp. 16–19.
[30] K.-W. Hsiao, J.-B. Huang, and H.-K. Chu, "Multi-view wire art," *ACM Trans. Graph.*, vol. 37, no. 6, pp. 1–11, Jan. 2019, doi: 10.1145/3272127.3275070.
[31] K. Sugihara, "Topology-disturbing objects: A new class of 3D optical illusion," *J. Math. Arts*, vol. 12, no. 1, pp. 2–18, Aug. 2017, doi: 10.1080/17513472.2017.1368133.
[32] K. Sugihara and M. Moriguchi, "Reflexively-fused cylinders," *Symmetry*, vol. 10, no. 7, pp. 1–9, Jul. 2018, doi: 10.3390/sym10070275.
[33] A. Shiraki, D. Matsumoto, R. Hirayama, H. Nakayama, T. Kakue, T. Shimobaba, and T. Ito, "Improvement of an algorithm for displaying multiple images in one space," *Appl. Opt.*, vol. 58, no. 5, pp. A1–A6, Jan. 2019, doi: 10.1364/AO.58.0000A1.
[34] *Standard Image/Sample Data*. Accessed: Jan. 18, 2022. [Online]. Available: http://www.ess.ic.kanagawa-it.ac.jp/app_images_j.html
[35] B. Huang and H. Ling, "End-to-end projector photometric compensation," in *Proc. IEEE/CVF Conf. Comput. Vis. Pattern Recognit. (CVPR)*, Jun. 2019, pp. 6803–6812, doi: 10.1109/CVPR.2019.00697.
[36] B. Huang and H. Ling, "CompenNet++: End-to-end full projector compensation," in *Proc. IEEE/CVF Int. Conf. Comput. Vis. (ICCV)*, Oct. 2019, pp. 7164–7173, doi: 10.1109/ICCV.2019.00726.

TOMOYA IMAMURA received the B.E. degree in engineering from Chiba University, Japan, in 2020. His research interest includes 3D systems and their applications.

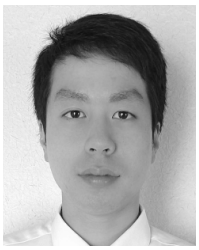

MITSURU BABA received the B.E. degree in engineering from the Kisarazu College, National Institute of Technology, Japan, in 2019, and the M.E. degree in engineering from Chiba University, Japan, in 2021. His research interest includes 3D systems and their applications.

NAOTO HOSHIKAWA (Member, IEEE) received the B.E. degree in engineering from Chiba University, in 2004, and the M.E. and Ph.D. degrees in information science from Nagoya University, in 2006 and 2012, respectively. He joined NTT EAST, in 2009, and was responsible for developing the server infrastructure for telecommunications services. He moved to the NTT Network Service Systems Laboratories, in 2013, to research and develop communication service systems and service infrastructures for IoT. From 2018 to 2019, he was an Assistant Professor with the National Institute of Technology, Oyama College, Japan, where he has been a Lecturer, from 2019 to 2021, where he has been an Associate Professor, since 2021. His research interests include information security, the IoT, network computing, and their service applications. He is a member of the IEICE and IPSJ.

HIROTAKA NAKAYAMA received the B.E., M.E., and Ph.D. degrees in engineering from Chiba University, in 2002, 2004, and 2011, respectively. He joined SQUARE ENIX, in 2004, and was in-charge of creating a background model for video games with interactive 3DCG. He moved to the National Astronomical Observatory of Japan as a Research Expert, in 2008, and is in-charge of scientific visualization and creating VR video by using visualized images. His research interests include image processing, computer graphics, stereoscopic visualization, and highly realistic displays. His awards and honors include the Animation Theater (SIGGRAPH Asia 2009), the Fulldome Short Film Competition First Award (International Festival of Scientific Visualization 2011), and the Creative Arts International Awards (AIS).

TOMOYOSHI ITO received the B.S. degree in pure and applied sciences and the M.S. and Ph.D. degrees in earth science and astronomy from The University of Tokyo, Japan, in 1989, 1991, and 1994, respectively. From 1992 to 1994, he was a Research Associate with Gunma University, Japan, where he was an Associate Professor, from 1994 to 1999. From 1999 to 2004, he was an Associate Professor with the Graduate School of Engineering, Chiba University, Japan, where he has been a Professor, since 2004. His research interests include high-performance computing and its applications, such as electronic holography for 3D TV. He is currently a member of ACM, ASJ, ITE, IEICE, IPSJ, and OSA.

ATSUSHI SHIRAKI received the B.E. degree in engineering from Yamaguchi University, Japan, in 2003, and the M.E. and Ph.D. degrees in engineering from Chiba University, Japan, in 2005 and 2008, respectively. From 2008 to 2011, he was an Assistant Professor with the National Institute of Technology, Kisarazu College, as a Lecturer, from 2011 to 2014, and an Associate Professor, from 2014 to 2015. Since 2015, he has been an Associate Professor with the Institute of Management and Information Technologies, Chiba University. His research interests include 3D systems, educational technology, and their applications. He is a member of ITE, IEICE, IPSJ, and JSET.